

Information entropic measures of a quantum harmonic oscillator under symmetric and asymmetric confinement within an impenetrable box

Abhisek Ghosal, Neetik Mukherjee and Amlan K. Roy*

Department of Chemical Sciences

Indian Institute of Science Education and Research (IISER) Kolkata,

Mohanpur-741246, Nadia,

West Bengal, India

Abstract

Information-based uncertainty measures like Shannon entropy, Onicescu energy and Fisher information (in position and momentum space) are employed to understand the effect of *symmetric and asymmetric* confinement in a quantum harmonic oscillator. In symmetric case, a wide range of confinement length (x_c) has been considered, whereas asymmetric confinement is followed by shifting the minimum of potential from origin keeping box length and boundary fixed. Eigenvalues and eigenvectors for these systems are obtained quite accurately via an imaginary time propagation scheme. One finds that, in symmetric confinement, after a certain characteristic x_c , all these properties converge to respective values of free harmonic oscillator. In asymmetric situation, excited-state energies always pass through a maximum. For this potential, the classical turning-point decreases, whereas well depth increases with the strength of asymmetry. Study of these uncertainty measures reveals that, localization increases with an increase of asymmetric parameter.

PACS Numbers: 03.65-w, 03.65Ca, 03.65Ta, 03.65.Ge, 03.67-a

Keywords:

*Corresponding author. Email: akroy@iiserkol.ac.in, akroy6k@gmail.com

I. INTRODUCTION

In recent years, instancy in studying spatially confined quantum systems has increased momentarily. In such small spatial dimensions, they exhibit many fascinating physical and chemical phenomena, in contrast to their corresponding *free unconfined* counterparts. This occurs mostly due to their complex energy spectra. These have potential applications in a wide range of problems, e.g., cell-model of liquid state, high-pressure physics, study of impurities in semiconductor materials, matrix isolated molecules, endohedral complexes of fullerenes, zeolites cages, helium droplets, nanobubbles, etc. Recent progress in nanotechnology has also inspired extensive research activity to explore and understand confined quantum systems (on a scale comparable to their de Broglie wave length). Their unique properties have been realized in a large array of quantum systems such as quantum wells, quantum wires, quantum dots as well as nanosized circuits (as in a quantum computer), and so forth, employing a wide variety of confining potentials. The literature is quite vast; interested reader is referred to a special issue and a book [1, 2], and references therein.

A significant amount of confinement work exists for model systems such as particle in a box, harmonic oscillator (HO), as well as real systems like H, He, other many-electron atoms, H_2^+ , H_2 and other molecules. At this point, it may be worthwhile to mention a few theoretical methods [3–15] employed for a 1D quantum HO (QHO) enclosed inside an impenetrable box, which is the subject matter of our current work. Some of the prominent ones are: a semiclassical WKB approximation [3, 10], a series analytical solution [4], perturbative, asymptotic and Padé approximant solutions [5], diagonal hypervirial [6], hypervirial perturbative [7], a Rayleigh-Ritz variation method with trigonometric basis functions [8], a numerical method [9], a perturbation method [11], power-series expansion [12], exact [13, 14] as well as highly accurate power-series solution [14], an imaginary-time propagation (ITP) technique [15], etc. While most of the works deal with the effect of boundary on energy levels, several other important properties such as dipole moment [11], Einstein's A, B coefficients [11, 12], magnetic effects [16, 17], effect of confinement size on non-classical statistical properties of coherent states [18] under high pressure, etc., were also followed by some researchers. Most of these works focus largely on *symmetrically* confined harmonic oscillator (SCHO); while the *asymmetrically* confined harmonic oscillator (ACHO) situation is treated only in a few occasions (such as [12, 15]).

It is well-known that, information entropy (IE)-based uncertainty measures, $S_x + S_p \geq 1 + \ln \pi$ (S_x, S_p denote Shannon entropies in position and momentum space), provide more rigorous and stronger bound than the conventional uncertainty product, $\Delta x \Delta p \geq \frac{\hbar}{2}$ (the symbols have usual significance). In quantum mechanics, position and momentum space are connected through uncertainty relation. Localization in position space leads to delocalization in momentum space and *vice versa*. In case of IE, measurements are carried out in both position and momentum space. The main interesting point in this respect, however, is that the extent of localization is not exactly same as delocalization in momentum space and *vice versa*. Thus a study of IE's in composite space provides a more complete information of the net localization-delocalization in a quantum system.

In the last decade, much light has been shed on the topic of IE in a multitude of systems, and this continues to go unabated, as evidenced by the large volume of literature available on the subject. For example, information measures, especially, Shannon entropy (S) in a decent number of physically and chemically important potentials have been reported lately. Some of the prominent ones are: Pöschl-Teller [19], Rosen-Morse [20], squared tangent well [21], hyperbolic [22], infinite circular well [23], hyperbolic double-well (DW) [24] potential, etc. In a recent publication [25], two of the present authors employed entropy measures like S , Fisher information (I), Onicescu energy (E) and Onicescu-Shannon information (OS) to analyze the competing effect of localization-delocalization in a *symmetric* DW potential, represented by, $V(x) = \alpha x^4 + \beta x^2 + \frac{\beta^2}{4\alpha}$. One finds quasi-degeneracy for certain values of the parameters α, β . Further, it was realized that, while traditional uncertainty relation and I were unable to explain such dual effects, measures like S and E were quite successful. In an analogous study [26], oscillation of a particle between larger and smaller wells were followed through information analysis in an *asymmetric* DW potential, given by, $V(x) = \alpha x^4 - \beta x^2 + \gamma x$. In this case, it was possible to frame some simple rules to predict quasi-degeneracy that occurs only for some characteristic values of the parameters present in the potential.

A vast majority of the IE-related works, referred above or otherwise, deal with the respective *free or unconfined* system. Such reports on quantum *confined* systems have been rather scarce and it would be highly desirable to follow their behavior as they may open up some new windows to explore. In a recent publication [27], S and traditional uncertainty relations were calculated and contrasted (significant differences were found in their behavior) in a SCHO model in position, momentum and phase space. In this follow-up, we wish to

extend our previous IE analysis for two celebrated model *confined quantum* systems, *viz.*, SCHO and ACHO inside an impenetrable 1D box. Thus at first, we examine the variation of energy as well as S , I and E in a SCHO, for small, intermediate and large confinement length (x_c) in position and momentum space. Next we consider similar changes in an ACHO, by shifting the potential minimum (d) keeping box length stationary. As mentioned earlier, the only IE analysis for a CHO, to the best of our knowledge, is through the Shannon entropy in case of SCHO. No such attempts are known for I , E , however. And so far, no work has been reported for similar entropic analysis in an ACHO. Thus, the present study can provide a more complete picture of the localization of bound stationary states of an enclosed system in position space and delocalization of the same in momentum space and *vice versa*. We also try to explain the result in an ACHO with Hellmann-Feynman [28] theorem taking d as a parameter. Additionally, classical turning points are calculated for ACHO as functions of d invoking the well-known semi-classical concept $|V(x) - \epsilon_n(d)| = 0$ [29], which can give further insight about the localization of particle in position space.

In order to facilitate further understanding, companion calculations are performed for phase-space area (A_n),

$$A_n = \int \sqrt{(V(x) - \epsilon_n)} dx, \quad (1)$$

as a function of length of confinement in SCHO and potential minimum in case of an ACHO. While IE gives a purely quantum mechanical viewpoint, this presents a semi-classical picture correlating IE and phase-space results. This may enable us to explain how box length and potential minimum impact tunneling and shape (nature) of phase space in such potentials.

In both cases, accurate eigenvalues and eigenfunctions of ground and excited states are obtained by employing an imaginary-time evolution method [15, 30–33]. It has been found to be quite successful for a variety of problems, including the confinement situation. The paper is organized as follows. In section II, a brief outline of ITP method and its implementation is presented; Section III offers a detailed discussion on IE for a boxed-in SCHO and ACHO in 1D. Finally Section V makes a few concluding remarks and future prospect.

II. METHOD OF CALCULATION

This section provides a brief account of the ITP method, which is applied here to obtain the eigenvalues and eigenfunctions of a caged-in quantum system inside an 1D impenetra-

ble box. It involves transformation of the respective time-dependent Schrödinger equation (TDSE) in imaginary time, to a non-linear diffusion equation. The latter is then solved numerically in conjunction with minimization of an expectation value to reach the lowest-energy state. By maintaining the orthogonality requirement with all lower states with same space and spin symmetry, higher states could be obtained sequentially. Since the method has been discussed at length earlier, here we give the essential details. For various other features, the reader may consult the references and therein.

The method is *in principle, exact* and was originally proposed several decade ago. It was utilized in a host of physical and chemical problems, e.g., random-walk simulation for *ab initio* SE for electronic systems, like H 2P , H $_3^+$ (D_{3h}) 1A_1 , H $_2$ $^3\Sigma_u^+$, H $_4$ $^1\Sigma_g^+$, Be 1S [34, 35]; by representing the Hamiltonian in grid a relaxation method was used for Morse potential, Hénon-Heiles system and weakly bound states of He on a Pt surface [36]; direct calculation of *ground-state* densities and other properties of rare gas atoms, molecules (H $_2$, HeH $^+$, He $_2^{++}$) through a TD quantum fluid dynamical density functional theory [31, 37, 38], *ground, excited* states of various 1D anharmonic DW [30], multiple-well [39], self-interacting [40], 2D DW potentials [32], etc. Also a finite difference time domain approach was also proposed for numerical solution of diffusion equation, which was applied to infinite square potential, harmonic oscillators in 1D, 2D, 3D as well as H atom, a charged particle in magnetic field, etc., [41–43]. The ITP method has also found applications in discretization of linear and non-linear SE by means of split-operator method [44], large-scale 2D eigenvalue problems in presence of magnetic field [45], and in several other situations [46–48].

Without any loss of generality, the non-relativistic TDSE for a particle trapped inside an 1D impenetrable box (atomic unit employed unless mentioned otherwise) can be written as,

$$i\frac{\partial}{\partial t}\psi(x,t) = H\psi(x,t) = \left[-\frac{1}{2}\frac{d^2}{dx^2} + v(x) + v_c(x) \right] \psi(x,t). \quad (2)$$

All the terms have usual significance. In present work, we consider the case of a harmonic oscillator, $v(x) = \frac{1}{2}k(x - d)^2$ (force constant k being kept fixed at unity throughout). For an SCHO and ACHO, $d = 0$ and $d \neq 0$ respectively. The desired confinement is achieved by enclosing the system inside two infinitely high hard walls:

$$v_c(x) = \begin{cases} 0, & -b < x < +b \\ +\infty, & |x| \geq b. \end{cases} \quad (3)$$

Figure (1) illustrates a SCHO for two box lengths 1, 2 respectively in left panel. Note that SCHO can be considered as an intermediate between particle in a box and a QHO. Next, we note that asymmetric confinement in a QHO can be accomplished in two ways: (i) changing the *box boundary*, keeping *box length* and potential minimum fixed at $d = 0$, (ii) the other way is to change d by keeping the *box length* and *box boundary* fixed. We have used the second condition; where an increase in d shifts the minimum towards right of origin, keeping box length, $b_2 - b_1 = 2$ constant, while the left and right boundaries are located at $b_1 = -1$, $b_2 = 1$ respectively. Furthermore, since $\frac{1}{2}k(x \pm d)^2$ represents a mirror-image pair confined within $-b_1$ to b_2 , their eigenspectra as well various expectation values are same for all states. Moreover the wave functions are mirror images of each other. Thus it suffices to study the behavior of any one of them; other one automatically follows from it. Right panel (b) of Fig. (1) shows a schematic representation of an ACHO potential, at five different d values.

Once can introduce a Wick rotational transformation from real time to imaginary time ($\tau = it$, where t denotes real time), to write Eq. (2) in following form,

$$-\frac{\partial\psi(x, \tau)}{\partial\tau} = H\psi(x, \tau), \quad (4)$$

whose formal solution can be written as follows,

$$\psi(x, \tau) = \sum_{k=0}^{\infty} c_k \phi_k(x) \exp(-\epsilon_k \tau). \quad (5)$$

Thus, taking $\epsilon_0 < \epsilon_1 < \epsilon_2 < \dots$, for large imaginary time, the wave function $\psi(x, \tau)$ will contain the lowest-energy (ground) state as dominating, i.e.,

$$\lim_{\tau \rightarrow \infty} \psi(x, \tau) \approx c_0 \psi_0(x) e^{-\epsilon_0 \tau}. \quad (6)$$

Hence if a initial trial wave function $\psi(x, \tau)$ at $\tau = 0$ is evolved for sufficiently long τ , one can reach the desired lowest-state energy. In other words, provided $c_0 \neq 0$, apart from a normalization constant, the global minimum corresponding to an expectation value $\langle \psi(x, \tau) | H | \psi(x, \tau) \rangle$ could be attained.

For the numerical solution of Eq. (4), one has to follow the time propagation of $\psi(x, \tau)$; this is achieved by invoking a Taylor series expansion of $\psi(x, \tau + \Delta\tau)$ around time τ ,

$$\psi(x, \tau + \Delta\tau) = e^{-\Delta\tau H} \psi(x, \tau). \quad (7)$$

This gives a prescription to advance the diffusion function $\psi(x, \tau)$ at an initial time τ to a future function $\psi(x, \tau + \Delta\tau)$ at time $\tau + \Delta\tau$. This is accomplished through the right-hand

Momentum-space wave functions are obtained from Fourier transform of their position-space counterparts; this is accomplished through standard FFT routines [50],

$$\phi(p) = \frac{1}{\sqrt{2\pi}} \int \psi(x) e^{ipx/\hbar} dx. \quad (11)$$

Next, we follow three information measures in this work. First of them is Shannon entropy [51], that signifies the expectation value of logarithmic probability density function. In position and momentum space, this is given by,

$$S_x = - \int \rho(x) \ln [\rho(x)] dx, \quad S_p = - \int \rho(p) \ln [\rho(p)] dp. \quad (12)$$

Total Shannon entropy (S), defined below, obeys the following bound,

$$S = S_x + S_p \geq (1 + \ln\pi). \quad (13)$$

Second one is Fisher information [52], which in position and momentum space, read as,

$$I_x = \int \left[\frac{|\nabla \rho(x)|^2}{\rho(x)} \right] dx, \quad I_p = \int \left[\frac{|\nabla \rho(p)|^2}{\rho(p)} \right] dp. \quad (14)$$

Net Fisher information, I , given as product of I_x and I_p , satisfies the following bound,

$$I = I_x I_p \geq 4. \quad (15)$$

The last one, Onicescu energy [53–55] is a rather recent development. This is expressed in position and momentum space as,

$$E_x = \int [|\rho(x)|^2] dx, \quad E_p = \int [|\rho(p)|^2] dp. \quad (16)$$

The corresponding total E is defined as,

$$E = E_x E_p \leq \frac{1}{2\pi}. \quad (17)$$

III. RESULTS AND DISCUSSION

A. Symmetric confinement

Since wave function, energy and some expectation values in a SCHO were discussed earlier (see, e.g., [5, 12, 14, 15]) in some detail, we do not report them in this work. Further,

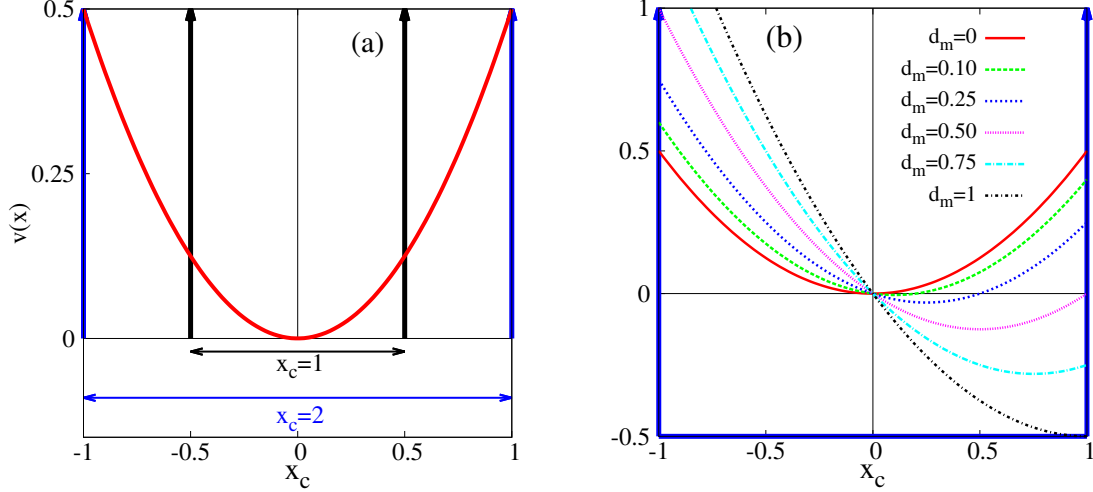


FIG. 1: Schematic representation of a confined QHO potential: (a) SCHO at two different box lengths 1 and 2 (b) ACHO at six different values of d .

a detailed discussion on accuracy and convergence of ITP eigenvalues, eigenfunctions with respect to grid parameters, in the context of confinement, has been provided in [15]; hence omitted here to avoid repetition. Thus, our primary focus is on information analysis. At the outset, it may be mentioned that, for *symmetric confinement*, some information theoretic (*Shannon entropy* only) measures in position, momentum and Wigner phase-space has been published [27]. However, to the best of our knowledge, no such attempt is known for I and E for a CHO. Thus the present work takes some inspiration from [27] and extends it further.

At first, Table 1 presents sample results for S_x , E_x for lowest five energy states of SCHO potential at three different x_c , *viz.*, 0.25, 2 and 5 covering small, intermediate and large regions. Several test calculations were performed on various number of grid points N , to check convergence. Generally, quality of the results improves as N increases and after some value, these remain practically unchanged. One can improve such results further by employing higher precision wave function on finer grid, present results are sufficiently accurate for the purpose at hand. Thus such calculations are not necessary in present context. For each of these quantities we also report the respective reference results, obtained by taking *exact* analytical eigenfunctions [13]. For even and odd states, these are given as:

$$\psi_e(x) = e^{-\frac{x^2}{2}} {}_1F_1\left(\frac{1}{4} - \frac{\epsilon_n}{2}, \frac{1}{2}, x^2\right), \quad \psi_o(x) = xe^{-\frac{x^2}{2}} {}_1F_1\left(\frac{3}{4} - \frac{\epsilon_n}{2}, \frac{3}{2}, x^2\right). \quad (18)$$

Here, ϵ_n and ${}_1F_1(a, b, x)$ denote energy eigenvalues and Kummer confluent hypergeometric function. The former is computed by putting confinement length $x = a$ and numerically

TABLE I: Calculated S_x^n, E_x^n or a SCHO at three selected confinement lengths, 0.25, 2 and 5, for five lowest states ($n = 0 - 4$). Reference results are obtained by taking *exact* analytical wave functions, reported in [13]. PR implies Present Result. See text for more details.

Property	$x_c = 0.25$		$x_c = 2$		$x_c = 5$	
	PR	Reference	PR	Reference	PR	Reference
S_x^0	-1.0000307	-1.0000307	0.9603491	0.9603491	1.0767572	1.0767573
S_x^1	-1.0000019	-1.0000019	1.0625421	1.0625421	1.3427276	1.3427277
S_x^2	-1.0000003	-1.0000003	1.0749785	1.0749785	1.4986081	1.4986082
S_x^3	-1.0000001	-1.0000001	1.0776239	1.0776239	1.6097006	1.6097006
S_x^4	-0.9999999	-0.9999999	1.0786018	1.0786018	1.6964625	1.6964627
E_x^0	3.0001200	3.0001200	0.4347289	0.4347291	0.3989422	0.3989422
E_x^1	3.0000070	3.0000075	0.3832620	0.3832622	0.2992065	0.2992067
E_x^2	3.0000010	3.0000014	0.3775775	0.3775772	0.2555729	0.2555724
E_x^3	3.0000005	3.0000005	0.3761693	0.3761693	0.2290809	0.2290810
E_x^4	3.0000001	3.0000001	0.3755618	0.3755620	0.2106059	0.2106061

solving following equations:

$${}_1F_1\left(\frac{1}{4} - \frac{\epsilon_n}{2}, \frac{1}{2}, a^2\right) = 0, \quad {}_1F_1\left(\frac{3}{4} - \frac{\epsilon_n}{2}, \frac{3}{2}, a^2\right) = 0 \quad (19)$$

for even, odd case respectively. In all cases, we notice that present results are practically coincident with those from reference. Note that, one can improve these results even further, if so desired, by employing higher precision wave function on finer grid. However, present results are sufficiently accurate for the purpose at hand; higher accuracy is not necessary in present context and not pursued any more. Similar conclusions hold for I_x .

Once the authenticity of ITP method is established, now we proceed for a detailed analysis on information measures. At first, Figure (2) shows the plots of S_x and S_p for five low-lying states. In panel (a), S_x increases with box length (indicating delocalization of particle) and converges to a constant value (S_x of QHO) at sufficiently large box length. Note that, at small x_c region, S_x changes insignificantly with state index n , resembling the behavior of so-called particle in a box problem, where S_x remains stationary with n . Next, panel (b), suggests that, S_p decreases with increase in box length and finally merges to corresponding QHO value. It is interesting to note that, there appears a minimum (becoming progressively more prominent as n increases) in excited state of S_p . Appearance of such minimum may be caused due to a competing effect in momentum space. Actually, three possibilities may be envisaged (l_x, l_p are box lengths at position, momentum space respectively):

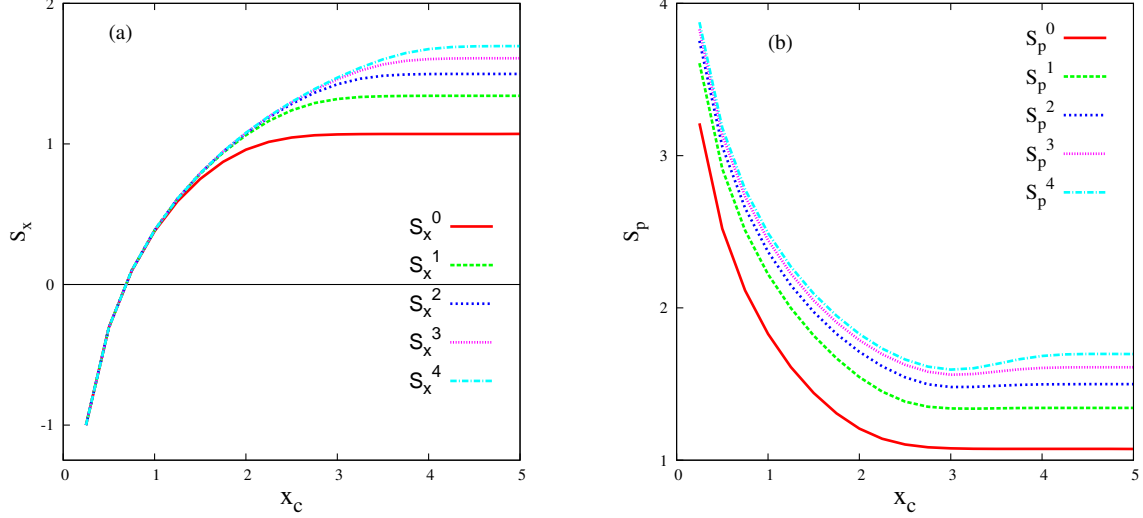


FIG. 2: Plot of S_x (a), S_p (b), of SCHO potential, as function of x_c , for first five energy states.

- (a) When $l_x \rightarrow 0$ then $l_p \rightarrow \infty$.
- (b) When l_x finite then l_p is also finite. But an increase in l_x leads to a decrease in l_p .
- (c) When $l_x \rightarrow \infty$ then also $l_p \rightarrow \infty$.

From above plots it is clear that, initially with increase in l_x , particle gets localized in momentum space (S_p decreases), but when potential starts behaving like QHO, de-localization occurs. Thus, existence of minimum in S_p is due to balance of two conjugate forces. Note that these variations of S_x , S_p as well the total quantity S (not presented here) with x_c are in harmony with the findings of [27].

Next we move on to the case of E and I , in a SCHO potential, which have not been studied before. whole calculation has been carried out in two different phases. First, we measure the position space localisation, momentum space delocalisation and coomposite space localisation-delocalisation of SCHO by computing I_x , E_x , I_p , E_p and I , E respectively. These calculation will also reinforce the conclusion obtained through the study of S_x , S_p and S in *Ref.* [3].

In second phase energy (ϵ_n), I_x , I_p & I , S_x , S_p & S and E_x , E_p & E are calculated for ACHO. In this calculation box length and box boundary has been fixed to 2.0 and -1 to 1 respectively. Here, we evaluate I , S , E and ϵ_n as a functional of potential minimum. Figure (3) shows classical turning point (L_{cl}) as a functional of d for first six energy states of ACHO. This result conclude that an increase in d leads to localisation in position space.

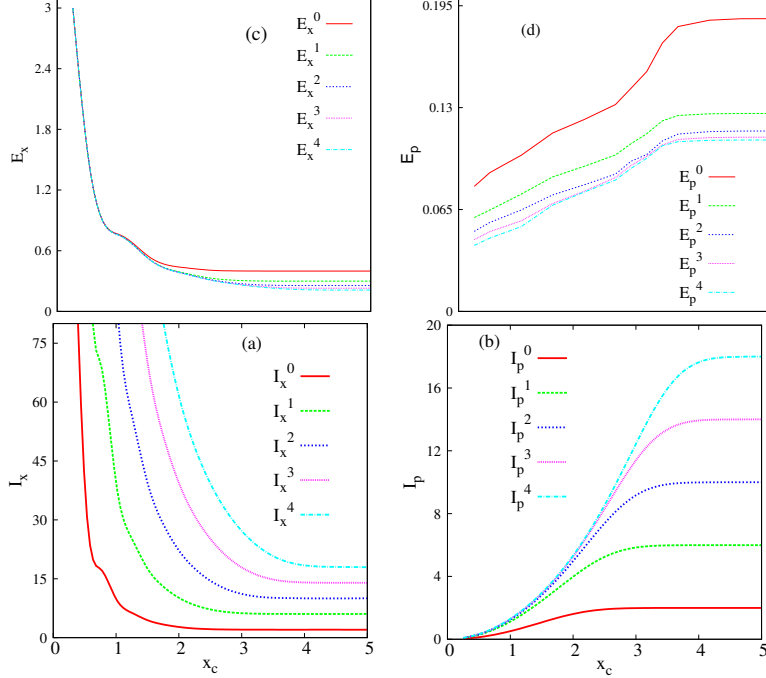


FIG. 3: Plot of I_x , I_p and E_x , E_p for first five energy states of SCHO potential as a function of x_c . Panels (a), (b), (c) and (d) represent I_x , I_p , E_x and E_p respectively.

Thus, it can be expected that, there will be delocalisation in momentum space. Initially, we have calculated ϵ_n and wave function for first six energy states. But, for further evaluation, we have restricted our calculation upto first five states.

The behavior of I_x and I_p of first five stationary-states are demonstrated in Fig: (4a) and (4b) respectively. Figure: (4a) shows that, I_x for all five states decreases with increase of x_c and finally converges to state-dependent constant values. At the same way, Fig: (4b) displays that, I_p for $n=0, 1, 2, 3, 4$ states increases with increase of x_c and margs to some state-dependent constant value. Figure: (5a) portrays that the appear a maximum in I at $n=2, 3, 4$ states. Appearance of such extremum in I concludes the competition of localisation-delocalisation feature. The I values in $n=0, 1, 2, 3$ states are larger for particle in a box model than the corosponding value for QHO.

It has been observed that, the nature of I_x , I_p & I is similar to the behavior of Δp , Δx , & $\Delta x \Delta p$ reported in *Ref.* [3]. These, results concludes that, SCHO can be considered as intermediate model between PIAB and QHO. Secondly, delocalisation in position space leads to decrease in I_x , whereas localisation in momentum space indicates an increase in I_p for SCHO.

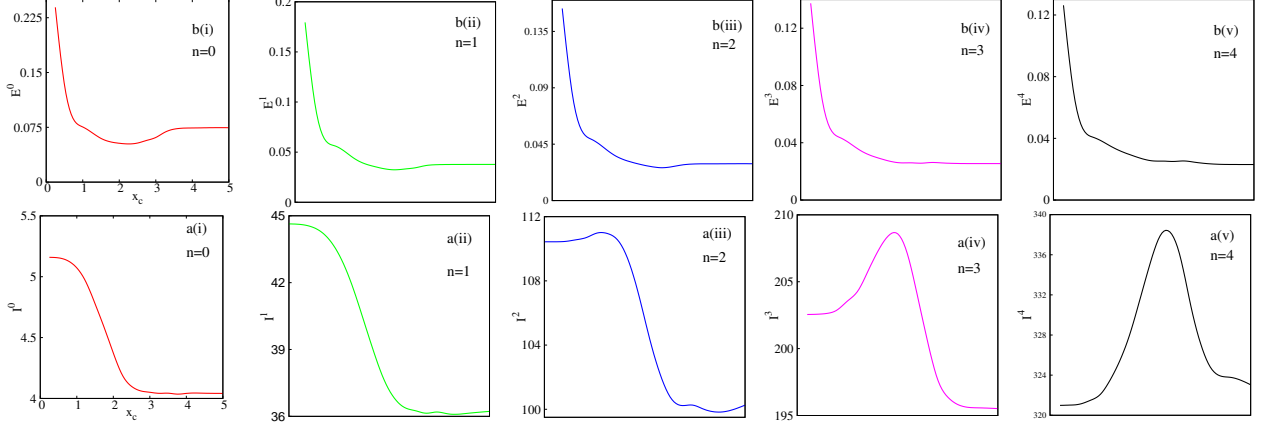


FIG. 4: Plot of I and E for first five energy states of SCHO potential as a function of x_c . Panel (a), (b) represent I and E respectively.

Figure: (4c) portrays that, E_x for all five states decreases with increase of confinement length indicating the delocalisation of the system. All these five values of E_x finally converges to some state dependent constant. It is interesting to note that, upto $x_c \approx 1$, E_x^n doesnot depend on quantum number. On the other hand, Fig: (4d) displays that, E_p increases with increase of x_c indicating the localisation of the system in momentum space. Figure: (5b) shows the variation of E as a function of x_c . In all five cases E decreases with increase of box length.

In study the effect of confinement in ACHO, we have to start from $d = 0$ which is actually the SCHO model.

B. Asymmetric confinement

Calculation for ACHO has been started by evaluating the energies of first six energy states as a functional of d . Figure: (6) shows the variation of ϵ_n as a functional of d for first six states. We have used variation induced exact diagonalisation method discussed in Ref. [21-22] to calculate the energy spectrum for larger d values ($d > 10$). In this calculation we employed the complete set of eigen functions of 1-D confined harmonic oscillator as the basis function. It has been found that for $n = 1, 2, 3, 4, 5$ states, ϵ_n passes through a maximum, only ϵ_0 decreases with increase of d . Hellmann-Feynman theorem was employed to explain the appearance of maximum. But, unfortunately, this theorem is not valid for confined quantum systems.

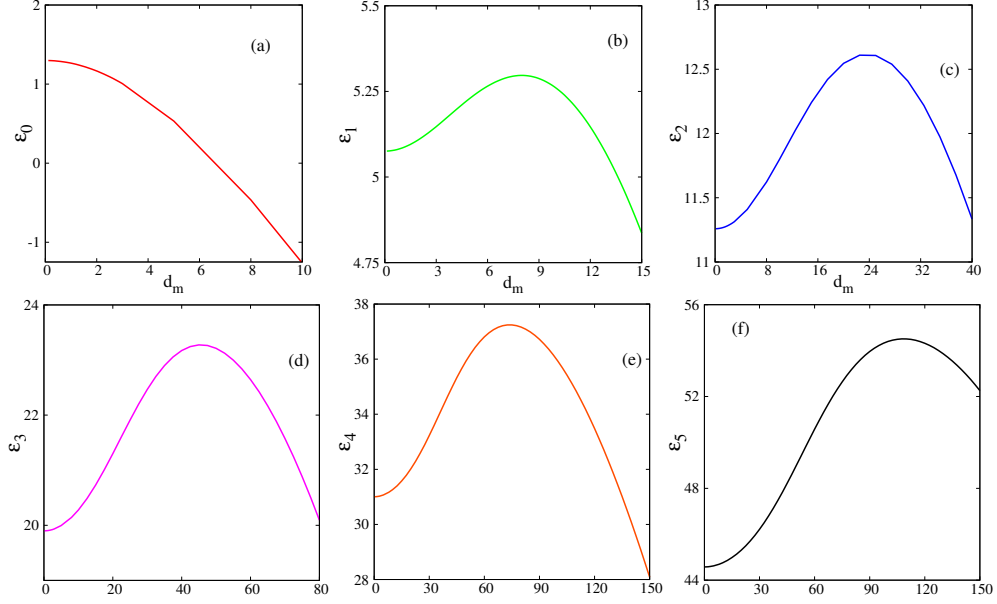


FIG. 5: Plot of energy values of first six energy states of ACHO potential as a function of d

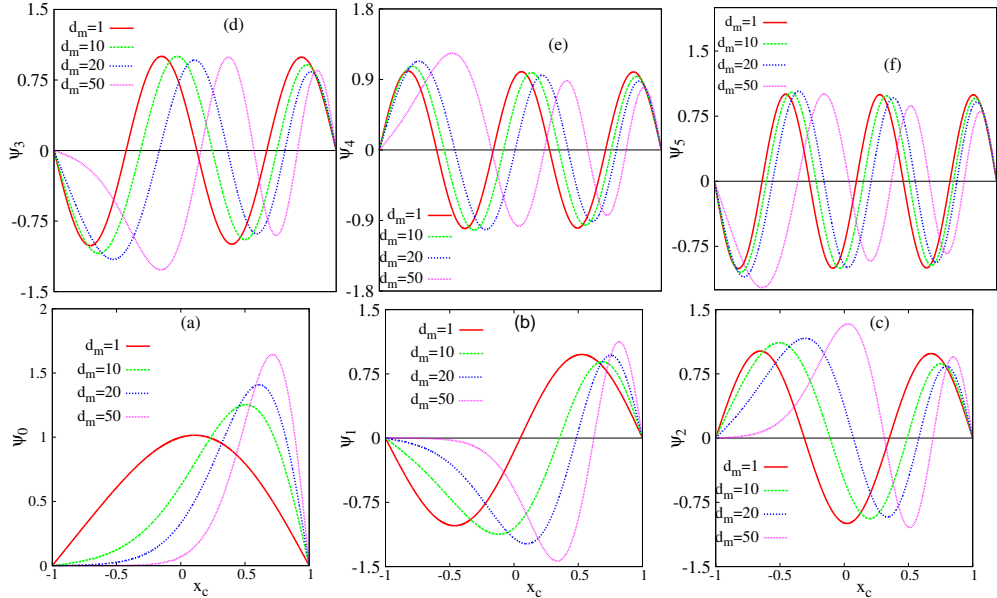


FIG. 6: Plot of wave function of first six energy states of ACHO potential at four different values of d namely 1, 10, 20, 50

Figure: (7 (a)-(f)) portrays the wave functions for first six energy states at four different values of d namely 1, 10, 20, 50. It is clear from Fig: (7) that, maximum, minimum and the nodal positions of all six wave functions shifted to the right with the increase of d . Analysis of the wave functions for all these six states indicate that, particle gets localised in position

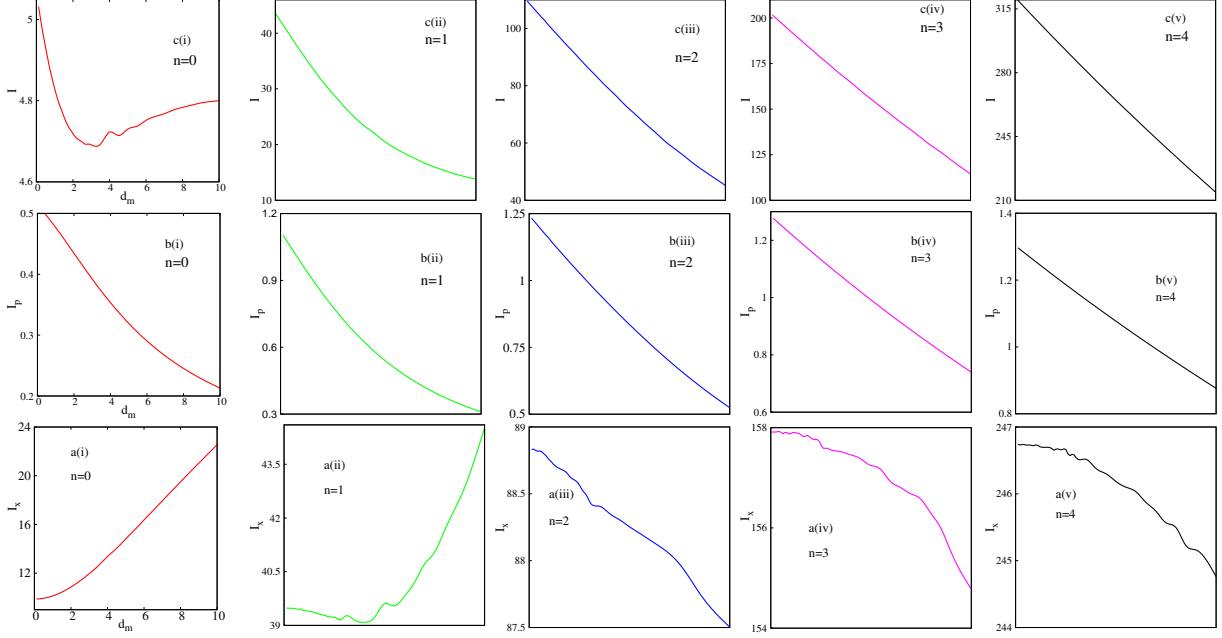


FIG. 7: Plot of I_x , I_p , I of first five energy states of ACHO potential as a function of potential minimum (d). Panels (a), (b), (c) represent I_x , I_p , I respectively.

TABLE II: I_x, I_p & I values for ground, first and second excited states of ACHO potential in Eq. (3) at five different values of d namely 0.12, 2.04, 5, 8 & 10.

d	I_x^0	I_p^0	I^0	I_x^1	I_p^1	I^1	I_x^2	I_p^2	I^2
0.12	9.8779	0.5094	5.0321	39.4817	1.1042	43.5969	88.8312	1.2333	109.5572
2.04	10.8976	0.4328	4.7160	39.2738	0.8476	33.2903	88.6558	1.0664	94.5478
5.0	14.8155	0.3192	4.7299	39.6028	0.55598	22.0184	87.6738	0.8353	73.2309
8.0	19.4987	0.2453	4.7836	41.6443	0.3826	15.9317	86.8009	0.6354	55.1564
10.0	22.5443	0.2129	4.7999	44.5216	0.3099	13.7968	86.2234	0.5242	45.2002

space with increase of d .

Figure: (8 (a)-(c)) delineate the style of I_x , I_p & I with variation of d respectively. Figure: (8a) shows that I_x for $n=0, 1$ states increases and for $n = 2, 3, 4$ decreases with increase of d . Thus, I_x for $n=0, 1$ states are able to indicate the localisation in position space. Study of Fig: (8b) reveal that, I_p for $n = 0, 1, 2, 3, 4$ states decreases with increase of d indicating the delocalisation of the system in momentum space. Further exploration disclose that, I for $n = 1, 2, 3, 4$ decreases with increase of d indicating net delocalisation in composite space. The appearance of minimum in I_0 may be due to the competition between localisation-delocalisation.

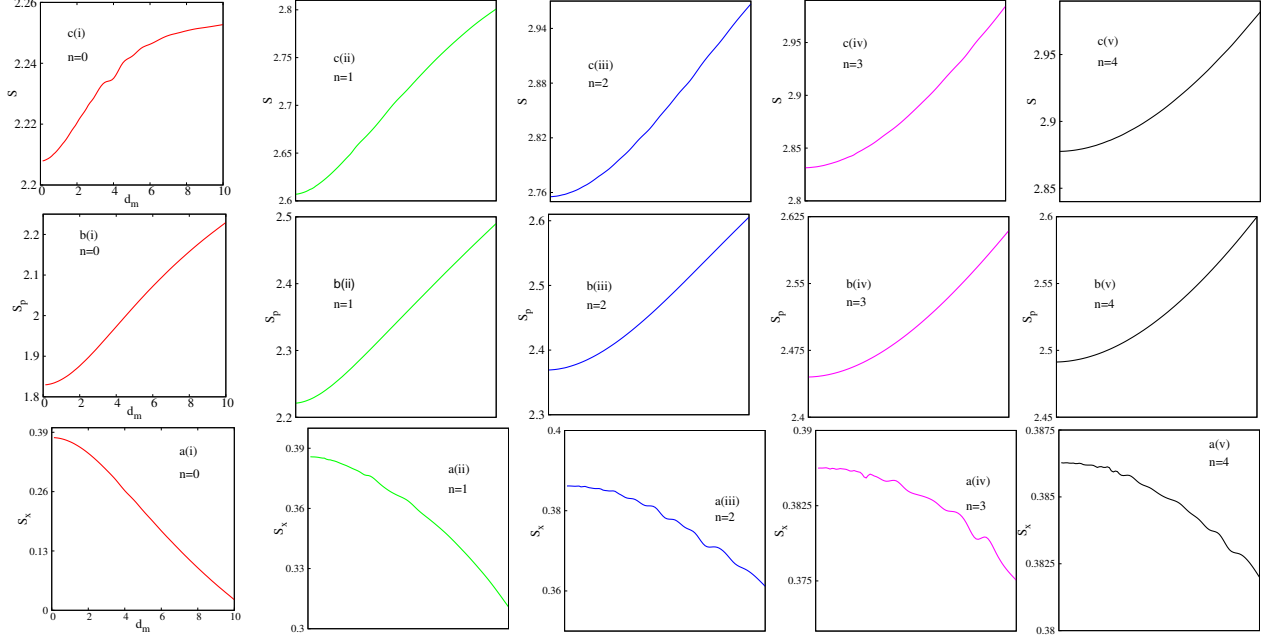


FIG. 8: Plot of S_x , S_p , S of first five energy states of ACHO potential as a function of potential minimum (d). Panels (a), (b), (c) represent S_x , S_p , S respectively.

TABLE III: S_x , S_p & S values for ground, first and second excited states of ACHO potential in Eq. (3) at five different values of d namely 0.12, 2.04, 5, 8 & 10.

d	S_x^0	S_p^0	S^0	S_x^1	S_p^1	S^1	S_x^2	S_p^2	S^2
0.12	0.3783	1.8296	2.2079	0.3857	2.2212	2.6069	0.3862	2.3692	2.7554
2.04	0.3428	1.8779	2.2208	0.3807	2.2512	2.6319	0.3850	2.3852	2.7703
5.0	0.2184	2.0238	2.2422	0.3636	2.3390	2.7027	0.3782	2.4512	2.8295
8.0	0.093	2.1576	2.2506	0.3360	2.4313	2.7674	0.3695	2.5429	2.9124
10.0	0.0233	2.2294	2.2527	0.3108	2.4900	2.8009	0.3611	2.6057	2.9668

It is necessary now to study the behavior of S_x , S_p & S as a functional of d . It is clear from Fig: (9a) that, S_x for all these five state decreases with increase of d , signifying the localisation of the particle in position space. Study of Fig: (9b) indicates that, S_p for all these five states increases with increase of d , explaining the delocalisation of the particle in momentum space. Figure: (9c) shows that, S for all the five states increases with increase of d . This observation indicates that, there is net delocalisation in composite position and momentum space (as the extent of delocalisation in momentum space is more than the extent of localisation in position space).

It can be seen from Fig: (10a) that, E_x for all the five states increases with increase of d

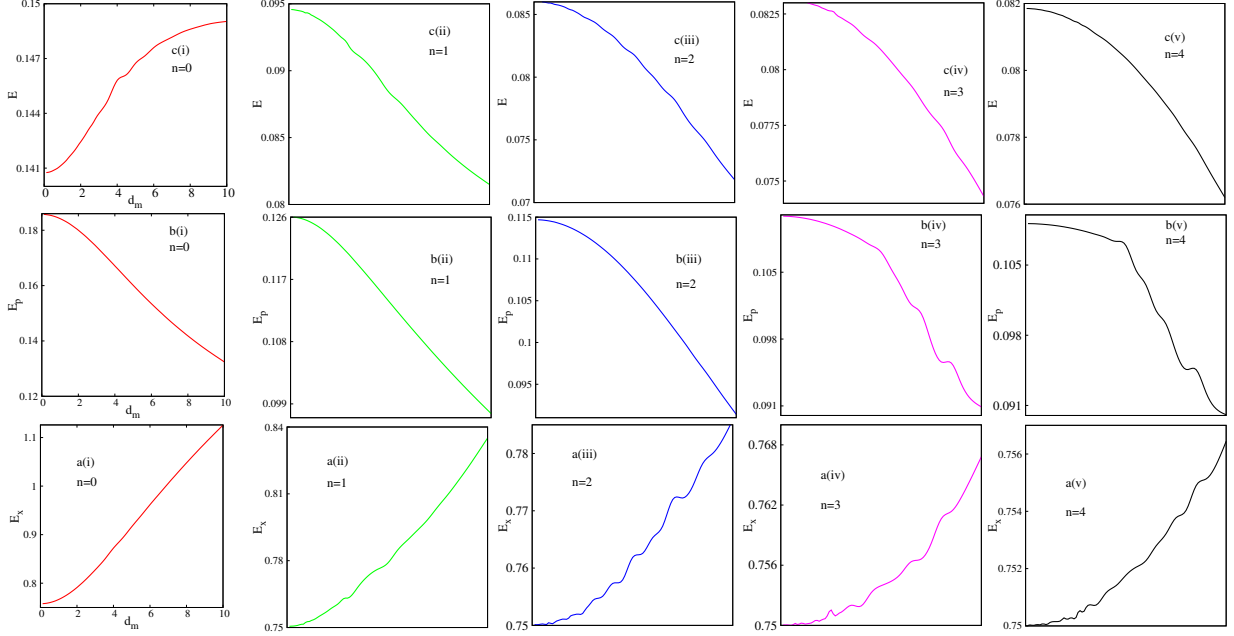


FIG. 9: Plot of E_x , E_p , E of first five energy states of ACHO potential as a function of potential minimum (d). Panels (a), (b), (c) represent E_x , E_p , E respectively.

illustrating the localisation in position space. Figure: (10b) demonstrates that, in case of all five states, E_p decreases with increase of d . Thus, E_p is able to explain the delocalisation in momentum space. Figure: (10c) shows that E for $n = 1, 2, 3, 4$ decreases with increase of d interpreting the net delocalisation in dualing space except E_0 increase with increase of d .

It is now clear that, only the study of S_x , S_p & S can completely explain the localisation-delocalisation phenomena in ACHO potentials. Study of E_x , E_p & E can also explain the dualing nature of the composite position and momentum space except for the ground state. But, the I_x , I_p & I are inconsistance to explain the conflicting effect in ACHO.

IV. CONCLUSION

Information based uncertainty measures like I , S & E has been evaluated to understand the effect of confinement of ACHO and SCHO. SCHO can be considered as an interim model between particle in a box model and quantum harmonic oscillator model. Whereas, one has to start from SCHO ($d = 0$) in order to study the effect of asymmetry in such systems. Here, I & E has been calculated for SCHO in position and momentum space. Study of I_x , I_p , I complements the conclusionas drawn from the study of Δx , Δp & $\Delta x \Delta p$.

In case of ACHO, an increase in d value leads to localisation in position space and delocalisation in momentum space. The study of S_x , S_p & S can completely explain these dualing phenomena in ACHO. But, unfortunately, study of I_x , I_p & I produces inconsistance results.

Extensive study of energies of first six states reveals that, Hellmann-Frynmann throrem is not valid for confined systems. Thus, additional corrections are necessary to apply such theorem in confined quantum systems.

Shannon entropy is capable to explain localisation-localisation effect in ACHO. It is noteworthy that, the study of effect of force constant in ACHO and SCHO will open a new domain in confined quantum systems. Further study of Wigner function using weyl transformation will disclose the effect of confinement in phase space. It is also necessary to establish a concrete relation between phase space entropy and composite position-momentum space entropy.

V. ACKNOWLEDGEMENT

AG is thankful to UGC for jounior research fellowship (JRF). NM acknowledges IISER Kolkata for a post-doctoral fellowship. It is a pleasure to thank Prof. A. K. Tiwari for constructive suggestions. Financial assistance from DST SERB () is gratefully acknowledged.

-
- [1] J. R. Sabin, E. Brändas and S. A. Cruz (Eds), *The Theory of Confined Quantum Systems*, Parts I and II, Advances in Quantum Chemistry, Vols. 57 and 58 (Academic Press, 2009).
 - [2] K. D. Sen (Ed.), *Electronic Structure of Quantum Confined Atoms and Molecules*, Springer (2014).
 - [3] R. Vawter, Phys. Rev. **174**, 749 (1968).
 - [4] R. Vawter, J. Math. Phys. **14**, 1864 (1973).
 - [5] V. C. Aguilera-Navarro, E. Ley Koo and A. H. Zimmerman, J. Phys. A **13**, 3585 (1980).
 - [6] F. M. Fernández and E. A. Castro, Int. J. Quant. Chem. **20**, 623 (1981).

- [7] G. A. Arteca, S. A. Maluendes, F. M. Fernández and E. A. Castro, *Int. J. Quant. Chem.* **24**, 169 (1983).
- [8] H. Taşeli, *Int. J. Quant. Chem.* **46**, 319 (1993).
- [9] R. Vargas, J. Garza and A. Vela, *Phys. Rev. E* **53**, 1954 (1996).
- [10] A. Sinha and R. Roychoudhury, *Int. J. Quant. Chem.* **73**, 497 (1999).
- [11] N. Aquino, E. Castaño, G. Campoy and V. Granados, *Eur. J. Phys.* **22**, 645 (2001).
- [12] G. Campoy, N. Aquino and V. D. Granados, *J. Phys. A* **35**, 4903 (2002).
- [13] H. E. Montgomery Jr., N. A. Aquino, K. D. Sen, *Int. J. Quantum Chem.* **107**, 798 (2007).
- [14] H. E. Montgomery Jr., G. Campoy and N. Aquino, *Phys. Scr.* **81**, 045010 (2010).
- [15] A. K. Roy, *Mod. Phys. Lett. A* **30**, 1550176 (2015).
- [16] Q. P. Li, K. Karrai, S. K. Yip, S. Das Sarma and H. D. Drew, *Phys. Rev. B* **43**, 5151 (1991).
- [17] D. Buchholz, P. S. Drouvelis and P. Schmelcher, *Phys. Rev. B* **73** 235346 (2006).
- [18] M. B. Harouni, R. Roknizadeh and M. H. Naderi, *J. Phys. A* **42**, 045403 (2009).
- [19] G.-H. Sun, M. A. Aoki and S. H. Dong, *Chin. Phys. B* **22**, 050302 (2013).
- [20] G.-H. Sun, S.-H. Dong and N. Saad, *Ann. Phys. (Berlin)* **525**, 934 (2013).
- [21] S. Dong, G.-H. Sun, S.-H. Dong and J. P. Draayer, *Phys. Lett. A* **378**, 124 (2014).
- [22] R. Valencia-Torres, G.-H. Sun and S.-H. Dong, *Phys. Scr.* **90**, 035205 (2015).
- [23] X.-D. Song, G.-H. Sun and S.-H. Dong, *Phys. Lett. A* **379**, 1402 (2015).
- [24] G.-H. Sun, S.-H. Dong, K. D. Launey, T. Dytrych and J. P. Draayer, *Int. J. Quant. Chem.* **115**, 891 (2015).
- [25] N. Mukherjee, A. Roy and A. K. Roy, *Ann. Phys. (Berlin)* **527**, 825 (2015).
- [26] N. Mukherjee and A. K. Roy, *Ann. Phys. (Berlin)* (in press).
- [27] H. G. Laguna and R. P. Sagar, *Ann. Phys. (Berlin)* **526**, 555 (2014).
- [28] I. N. Levine, *Quantum Chemistry*, Pearson Prentice Hall, New Jersey, 2009.
- [29] D. J. Griffiths and E. G. Harris, *Introduction to Quantum Mechanics*, Pearson Prentice Hall, New Jersey, 2004.
- [30] A. K. Roy, N. Gupta, and B. M. Deb, *Phys. Rev. A* **65**, 012109 (2002).
- [31] A. K. Roy, S. I. Chu, *J. Phys. B* **35**, 2075 (2002).
- [32] A. K. Roy, A. J. Thakkar and B. M. Deb, *J. Phys. A* **38**, 2189 (2005).
- [33] A. K. Roy, *J. Math. Chem.* **52**, 2645 (2014).
- [34] J. B. Anderson, *J. Chem. Phys.* **63**, 1499 (1975).

- [35] D. R. Garmer and J. B. Anderson, *J. Chem. Phys.* **86**, 4025 (1987).
- [36] R. Kosloff and H. Tal-Ezer, *Chem. Phys. Lett.* **127**, 223 (1986).
- [37] B. K. Dey and B. M. Deb, *J. Chem. Phys.* **110**, 6229 (1999).
- [38] A. K. Roy, B. K. Dey and B. M. Deb, *Chem. Phys. Lett.* **308**, 523 (1999).
- [39] N. Gupta, A. K. Roy and B. M. Deb, *Pramana J. Phys.* **59**, 575 (2002).
- [40] A. Wadehra, A. K. Roy and B. M. Deb, *Int. J. Quant. Chem.* **91**, 597 (2003).
- [41] I. W. Sudiarta and D. J. Wallace Geldart, *J. Phys. A* **40**, 1885 (2007).
- [42] I. W. Sudiarta and D. J. Wallace Geldart, *Phys. Lett. A* **372**, 3145 (2008).
- [43] I. W. Sudiarta and D. J. Wallace Geldart, *J. Phys. A* **42**, 285002 (2009).
- [44] L. Lehtovaara, J. Toivanen and J. Eloranta, *J. Comput. Phys.* **221**, 148 (2007).
- [45] P. J. J. Luukko and E. Räsänen, *Comput. Phys. Commun.* **184**, 769 (2013).
- [46] M. Aichinger, S. A. Chin and E. Krotscheck, *Chem. Phys. Lett.* **470**, 342 (2005).
- [47] S. A. Chin, S. Janecek and E. Krotscheck, *Chem. Phys. Lett.* **470**, 342 (2009).
- [48] M. Strickland and D. Yager-Elorriaga, *J. Comput. Phys.* **229**, 6015 (2010).
- [49] <http://www.math.uakron.edu/~kreider/anpde/Anpde.html>.
- [50] M. Frigo and S. G. Johnson, *Proc. IEEE* **93**, 216 (2005).
- [51] C. E. Shannon, *Bell Sys. Tech. J.* **30**, 50 (1951).
- [52] T. M. Cover and J. A. Thomas, *Elements of Information Theory* (John Wiley & Sons, Hoboken, NJ, 2006).
- [53] K. Ch. Chatzisavvas, Ch. C. Moustakidis and C. P. Panos, *J. Chem. Phys.* **123**, 174111 (2005).
- [54] M. Alipour and A. Mohajeri, *Mol. Phys.* **110**, 403 (2012).
- [55] M. Agop, A. Gavriluț and E. Rezuș, *Int. J. Mod. Phys. B* **29**, 1550045 (2015).
- [56] N. Aquino, V. Granados, H. Yee-Madeira, *Rev. Mex. Fis.* **55** 125 (2009).
- [57] N. Aquino, G. Campoy, H. E. Montgomery, *Int. J. Quantum Chem.* **107** 1548 (2007).
- [58] G. Campoy, N. Aquino and V. D. Granados, *J. Phys. A: Math. Gen.* **35** 4903 (2002).
- [59] G. Yañez-Navarro, G.-H. Sun, T. Dytrych, K. D. Launey, S.-H. Dong and J. P. Draayer, *Ann. Phys.* **348**, 153 (2014).
- [60] G.-H. Sun, P. Duan, C.-N. Oscar and S.-H. Dong, *Chin. Phys. B* **24**, 100303 (2015).
- [61] B. L. Hammond, W. A. Lester Jr. and P. J. Reynolds, *Monte Carlo Methods in Ab Initio Quantum Chemistry*, World Scientific, 1994.
- [62] (Eds.) M. Abramowitz and I. Stegun, *Handbook of Mathematical Functions*, Dover, 1964.

- [63] R. López-Ruiz, H. L. Mancini and X. Calbet, Phys. Lett. A **209**, 321 (1995).
- [64] C. P. Panos, K. Ch. Chatzisavvas, Ch. C. Moustakidis and E. G. Kyrkou, Phys. Lett. A **363**, 78 (2007).
- [65] L. J. Stevanović and K. D Sen, J. Phys. B **41**, 225002 (2008).

